



La Science à l'œuvre pour le
at work for Canada

NRC Publications Archive (NPArc) Archives des publications du CNRC (NPArc)

Numerical modelling of PAH formation and soot inception in the central/pyrolysis region of an ethylene/air diffusion flame

Dworkin, Seth B.; Zhang, Qingang; Guo, Hongsheng; Liu, Fengshan; Smallwood, Gregory J.; Thomson, Murray J.

Web page / page Web

<http://nparc.cisti-icist.nrc-cnrc.gc.ca/npsi/ctrl?action=rtdoc&an=16239506&lang=en>
<http://nparc.cisti-icist.nrc-cnrc.gc.ca/npsi/ctrl?action=rtdoc&an=16239506&lang=fr>

Access and use of this website and the material on it are subject to the Terms and Conditions set forth at
http://nparc.cisti-icist.nrc-cnrc.gc.ca/npsi/jsp/nparc_cp.jsp?lang=en

READ THESE TERMS AND CONDITIONS CAREFULLY BEFORE USING THIS WEBSITE.

L'accès à ce site Web et l'utilisation de son contenu sont assujettis aux conditions présentées dans le site

http://nparc.cisti-icist.nrc-cnrc.gc.ca/npsi/jsp/nparc_cp.jsp?lang=fr

LISEZ CES CONDITIONS ATTENTIVEMENT AVANT D'UTILISER CE SITE WEB.

Contact us / Contactez nous: nparc.cisti@nrc-cnrc.gc.ca.



National Research
Council Canada

Conseil national
de recherches Canada

Canada

Numerical Modelling of PAH Formation and Soot Inception in the Central/Pyrolysis Region of an Ethylene/Air Diffusion Flame

Seth B. Dworkin^{a*}, Qingan Zhang^a, Hongsheng Guo^b, Fengshan Liu^b, Gregory J. Smallwood^b,
Murray J. Thomson^a

^a*Dept. of Mechanical and Industrial Engineering, Univ. of Toronto, 5 King's College Road, Toronto, ON, M5S 3G8*

^b*Inst. for Chemical Process and Env. Technology, National Research Council of Canada, Building M-9, 1200
Montreal Road, Ottawa, ON, K1A 0R6*

1. Introduction

High concentrations of combustion-generated soot in the atmosphere are known to pose significant health risks, cause cloud and contrail formation, and contribute to long-term global climate change. Although much progress has been made, a complete understanding of soot formation in combustion still eludes researchers. In order to accurately model soot formation in combustion simulation algorithms, numerous mechanisms which contribute to overall soot concentration need to be considered. These include particle inception, coalescence, surface growth, oxidation, and Polycyclic Aromatic Hydrocarbon (PAH) condensation [1]. Some of these processes, in particular soot particle inception, are poorly understood and difficult to model. Inception depends on local concentrations of aromatic species, the size of which depend on the fuel being burned [1-3]. The chemical kinetics of these large molecules involve hundreds of intermediate chemical species and thousands of reaction steps [4,5]. For this reason, detailed PAH-based soot inception modelling is computationally expensive, and has often been approximated in multidimensional chemically reacting flow problems.

Recent developments in parallel algorithms [6-8] coupled with the increasing availability of faster and more affordable computer processing units have led to scalable simulation algorithms that are capable of simulating a new realm of problems. Although parallelization has led to more detailed models for soot formation, and some quantitative accuracy, no universally-applicable soot model exists, which is capable of predicting soot levels in each of premixed flames, non-premixed flames, and pyrolysis reactors. One key modelling deficiency, that has been reported by numerous researchers, is the difficulty in accurately modelling soot formation in the central/pyrolysis region of non-premixed flames [6,7,9]. In this region, rich fuel pyrolysis occurs via heating from the hotter annular regions of the flame. The PAHs that lead to soot inception are formed at relatively low temperatures in this region, and lead to substantial soot concentrations that are typically underpredicted by numerical models.

In the present work, an efficient distributed-memory parallel solver enables the testing of a variety of assumptions that have been commonly made in soot modelling, and their effect on centerline soot formation. In an attempt to reconcile a commonly-used soot model that accurately predicts peak soot concentrations in non-premixed flames, with underpredicted coflow flame centerline soot concentrations, three assumptions are tested: 1. Neglecting species thermal diffusion may lead to an underprediction of PAH concentrations along the centerline since thermal diffusion is known to cause large molecules to diffuse down a temperature gradient, away from the hotter annular region of the flame, and may result in an underprediction of soot inception rates in the central/pyrolysis region. Thermal diffusion has been shown in the literature to have an effect on soot profiles by changing PAH and hydrogen distributions within the flame [10]; 2. Considering inception only via PAH growth neglects the growth of polyne chain molecules, which have been shown to lead to soot inception for some fuels in pyrolysis reactors [11]; 3. The chemical kinetic mechanisms for PAH growth typically neglect all formation pathways other than Hydrogen Abstraction Carbon Addition (HACA) via acetylene. Some additional formation pathways including propargyl addition [12] and cyclopentadiene combination [13] have been shown to contribute to PAH growth in some systems.

2. Parallel Flame Solver and Combustion Conditions

2.1 Rich Non-Premixed Flame and Solution Algorithm

The first flame to be studied is the steady, atmospheric pressure, laminar sooting coflow ethylene/air diffusion flame first studied by Santoro and coworkers, described in [14]. For the computations, the fully-coupled

* Corresponding author: sdworkin@mie.utoronto.ca

elliptic steady conservation equations for mass, momentum, energy, species mass fractions, soot aggregate number densities, and primary particle number densities are solved in a two-dimensional axisymmetric cylindrical coordinate system. A detailed description of the governing equations, boundary conditions and solution methodology can be found in [6,7,15].

The sectional soot model considers nucleation based on the collisions of two pyrene molecules in the free-molecular regime, surface growth, PAH surface condensation, coagulation, fragmentation, particle diffusion, and thermophoresis. The mass range of soot aggregates is divided logarithmically into thirty-five discrete sections, each with a prescribed representative mass [16]. Surface growth is calculated by the Hydrogen Abstraction Carbon Addition (HACA) mechanism developed in [4,17,18,19].

The soot model accounts for PAH condensation by considering collisions between pyrene molecules and soot aggregates [4]. The probability of sticking in each collision is assumed to be 0.55 [15]. Radiation by soot, H₂O, CO₂, and CO is calculated using the discrete-ordinates method and a statistical narrow-band correlated-k-based model [20]. The base chemical kinetic mechanism used here is that of Appel *et al.* [4] for PAH growth and pyrene formation. To test the effect of polyene-based inception, and alternative PAH growth routes, chemical species and reactions are appended to the chemical mechanism of Appel *et al.* [4] as described in the following section.

A finite volume method is used to discretize the governing equations over a staggered mesh, which are solved using a semi-implicit algorithm [6,7,21]. Pseudo-transient continuation is used to aid convergence from an arbitrary starting estimate. The thermal properties of the gaseous species and chemical reaction rates are obtained using CHEMKIN subroutines [22,23]. Transport properties which include mixture-averaged quantities for viscosities, conductivities, and diffusion coefficients, as well as thermal diffusion coefficients for H and H₂, are evaluated using TPLIB [24,25]. When testing the effect of thermal diffusion, TPLIB is used to calculate thermal diffusion coefficients for all chemical species present in the mechanism.

2.2 *Opposed Flow Diffusion Flame*

The simplified one-dimensional model of an opposed jet diffusion flame can prove to be very instructional in understanding chemical phenomena. The effects of adding new growth pathways to the chemical mechanism on PAH concentrations can be preliminarily assessed in the one-dimensional opposed flow geometry without soot formation [26]. The highly detailed experimental data set of Olten and Senkan [27] is used for comparison as it contains measurements of bulk flame properties such as temperature and major species profiles, but also PAH concentration profiles, for an ethylene diffusion flame of interest in the present work. By comparing computational data for PAH profiles to this experimental data set, it can be determined whether changes to the PAH growth chemistry improve or worsen their correlation to experimental data.

Opposed flow diffusion flame solutions are computed using the commercial software package, Chemkin Pro™ [28]. The flame conditions studied in [27] are easily implemented in Chemkin Pro™ and are used in the present work. They are detailed in the following section.

2.3 *Non-Premixed Diluted Diffusion Flame*

A third flame is studied that is very similar to the flame described in Section 2.1, with the main difference being that the fuel stream is heavily diluted with nitrogen. In addition, the flow in this case is confined by a 10.8-cm-inner-diameter concentric chimney. This system is chosen because of the availability of experimental data for centerline PAH and soot concentrations [29]. By comparing computational data for PAH and soot centerline profiles to the experimental data set in [29], it can be determined whether changes to the PAH growth chemistry improve or worsen the PAH and soot concentration profiles. Since a similar study is undertaken with the opposed flow diffusion flame described in Section 2.2, this study can also shed light on the interaction of simplified one-dimensional flame modelling with the more complex coflow flame geometry. The computational algorithm used for this component of the study is the same as that described in detail in Section 2.1. Changes that are made to match the experimental conditions are detailed in the following section.

3. Results and Discussion

3.1 *Effect of Thermal Diffusion*

A “base” computation is performed of an ethylene/air coflow diffusion flame on a coannular burner. Since the flame is axisymmetric, it can be modelled as a two-dimensional problem. A non-uniform mesh is used to save computational cost while still resolving large spatial gradients. Flat velocity profiles are assumed for the inlet fuel and oxidizer streams, at 3.98 cm/s and 8.90 cm/s, to match the flow rates in [14]. The inlet temperatures for fuel and oxidizer are set to 300 K. Symmetry, free-slip, and zero-gradient conditions are enforced at the centerline, the outer radial boundary, and the outflow boundary, respectively. The computational domain is divided uniformly into 192 subdomains with the boundaries of each subdomain perpendicular to the *z*-axis. This model is one for which it has

been reported that soot concentrations are significantly underpredicted along the flame centerline, despite good agreement between computation and experiment in the annular region of the flame [15]. The computation required approximately 25,000 timesteps, at 19 seconds each, totalling just under six days. Contour plots of temperature and soot volume fraction are shown in Fig. 1.(a) and (b), respectively. The computed flame is slightly lifted and reaches a temperature of 2055 K. Most of the soot is formed on the wings of the flame, just downstream of the hottest regions. The peak predicted soot volume fraction is 8.8 ppm, which is consistent with the experimental data [15].

A second computation is performed that is otherwise identical except for the inclusion of thermal diffusion velocities for all species. This requires inversion of a full transport matrix, and adds significant computational cost. This computation required 54 seconds per timestep, making it three times more computationally expensive.

Figure 1.(c) shows the computed centerline pyrene mole fractions for the base computation and the computation with thermal diffusion (TD). Pyrene, the incepting PAH in the model, is slightly lower along the centerline when thermal diffusion is included. Pyrene, a comparatively heavy species, is being driven away from the central region of the flame by thermal diffusion. Although there are decreasing temperature gradients toward the centerline (see Fig. 1.(a)), the net effect of thermal diffusion is to decrease centerline pyrene concentration. As a result, computed soot volume fraction, shown in Fig 1.(d) follows the same trend as pyrene by decreasing as well.

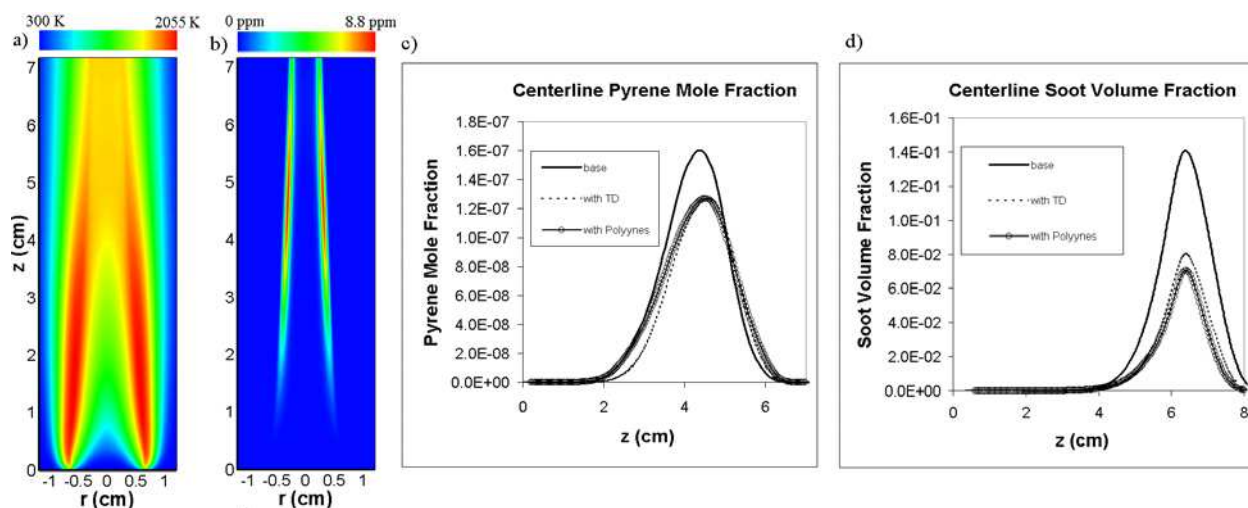


Fig. 1. a) Computational isotherms for the “base” flame. b) Computational isopleths of soot volume fraction for the “base” flame. c) Centerline pyrene concentrations for the “base” computation, the computation with thermal diffusion (TD), and the computation with polyne chemistry. d) Centerline soot volume fraction profiles for the “base” computation, the computation with thermal diffusion (TD), and the computation with polyne chemistry.

3.2 Effect of Polyne-Based inception

It has been reported by some researchers (see, for example, [11]) that considering polyne-based inception is necessary to accurately model soot formation in shock tube/pyrolysis systems. Due to the thermophysical similarity between shock tube/pyrolysis systems and the central/pyrolysis region of a coflow diffusion flame, it is postulated that neglecting polyne-based inception could be responsible for the underprediction of soot formation in this region. To test this assumption, a computation is performed that is otherwise identical to the “base” calculation except for the inclusion of a detailed polyne growth and inception model taken from [11]. The additional computational cost of including polyne chemistry was negligible. The results of the computations are shown in Fig. 1.(c) and (d).

The effect of adding polyne-based inception on centerline pyrene concentrations and soot volume fraction was similar to that of adding thermal diffusion. Pyrene and polyne chemistry are linked through acetylene. Adding polyne chemistry has diverted acetylene into polyne growth and away from pyrene growth, thus decreasing pyrene concentrations along the centerline, as can be seen in Fig. 1.(c). The augmentation in soot inception from the consideration of polyynes has been more than offset by the decrease in pyrene, the principal incepting species, resulting in a net decrease in soot volume fraction along the centerline, as shown in Fig. 1.(d).

3.3 Effect of PAH growth

The effect of two commonly neglected PAH growth pathways is first tested in the one-dimensional counterflow geometry. The flame conditions used in [27] are modelled in Chemkin ProTM and the results are

compared with the experimental data set. A “base” computation is first performed using the chemical mechanism of Appel *et al.* [4], which considers only acetylene addition (HACA growth) for aromatics from benzene to pyrene. The fuel stream contains 75% ethylene and 25% argon and issues from a 2.54 cm inner diameter jet at a velocity of 13.16 cm/s. The oxidizer stream contains 22% oxygen and 78% argon and issues from an identical burner at a velocity of 16.12 cm/s. The fuel and oxidizer ports are separated by 1.5 cm.

A second computation is performed with an augmented chemical kinetic mechanism. This chemistry set couples to the PAH growth reactions of D’Anna and Kent [12] to the fuel oxidation kinetics of Appel *et al.* [4]. The new PAH growth mechanism considers HACA growth, cyclopentadiene combination, cyclopentadiene-indene combination, and propargyl addition. The results of these computations are shown in Fig. 2.

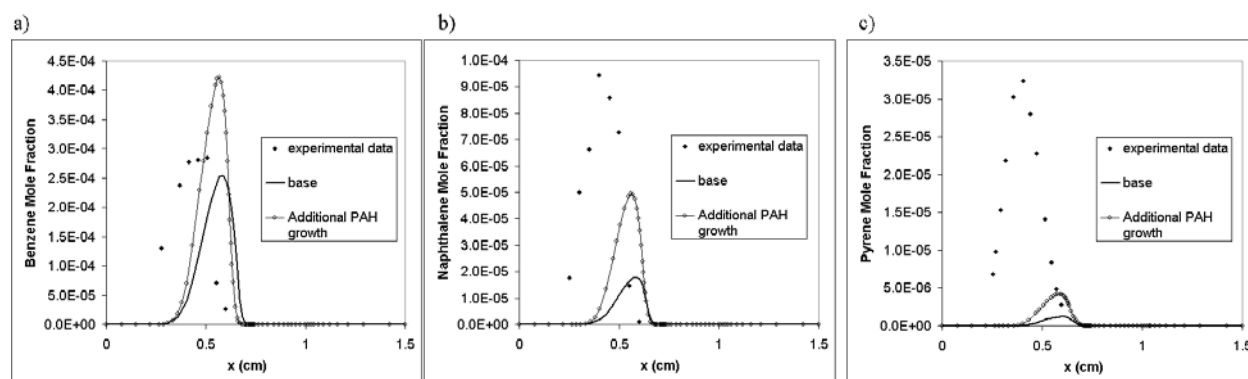


Fig. 2. Comparison of experimental and computed mole fractions for the “base” model and the model with additional PAH growth pathways: a) benzene, b) naphthalene, and c) pyrene.

Figure 2.(a) shows that the benzene profiles predicted by both the base and augmented mechanisms agree well with experimental data. The peak benzene mole fraction predicted by the augmented mechanism is much higher than that of the base mechanism but both are within experimental uncertainty. Both mechanisms predict peak benzene being formed closer to the fuel inlet than is measured. In the computed naphthalene profiles (Fig. 2.(b)), the change is more dramatic. The base mechanism significantly underpredicts naphthalene mole fraction whereas the augmented mechanism results in more than doubling of the peak naphthalene concentrations, and a profile much closer to the experimentally measured values. This result is significant given the consistent underprediction in soot formation mentioned earlier. The augmented mechanism leads to a similar increase in pyrene concentrations over those predicted by the base mechanism (Fig. 2.(c)). Despite this increase, however, the profile is still underpredicted by an order of magnitude when compared to the experimental data.

To gauge the effect that these new PAH growth pathways might have on PAH and soot formation in the central/pyrolysis region of a coflow diffusion flame, the new combined mechanism is implemented into the parallel coflow diffusion flame solver. Here, the confined non-premixed flame of McEnally and Pfefferle [29] is modelled due to the unique availability of experimental data for both PAH and soot concentrations along the centerline.

A new “base” computation is first performed using the chemical mechanism of Appel *et al.* [4]. Flat velocity profiles are assumed for the inlet fuel and oxidizer streams, at 12.5 cm/s and 32.6 cm/s, respectively, to match the flow rates in [29]. Based on reported temperature measurements, the inlet temperatures for fuel and oxidizer are set to 400 K and 300 K, respectively. Symmetry, no-slip, and zero-gradient conditions are enforced at the centerline, the outer radial boundary, and the outflow boundary, respectively. The computational strategy is otherwise the same as that described in Section 3.1.

A second computation is performed that is identical except for use of the PAH growth reactions of D’Anna and Kent [12] that not only consider HACA growth of PAHs but also consider cyclopentadiene combination, cyclopentadiene-indene combination, and propargyl addition. The results of these computations are shown in Fig. 3. From Fig. 3.(a), it can be seen that use of the augmented mechanism results in a significant increase in benzene mole fraction along the centerline as compared to the base run. The data from the augmented mechanism is also much closer to the experimental data. A similar trend can be seen in the predicted naphthalene mole fractions from Fig. 3.(b). Again, the naphthalene mole fractions predicted using the augmented mechanism were much closer to the experimental data. For both species, however, the augmented mechanism still underpredicts the measured mole fractions quite significantly – by about a factor of two. Although the increased PAH growth leads to nearly a doubling of soot formation along the centerline, the predicted soot concentrations are still an order of magnitude less than the measured quantities [15].

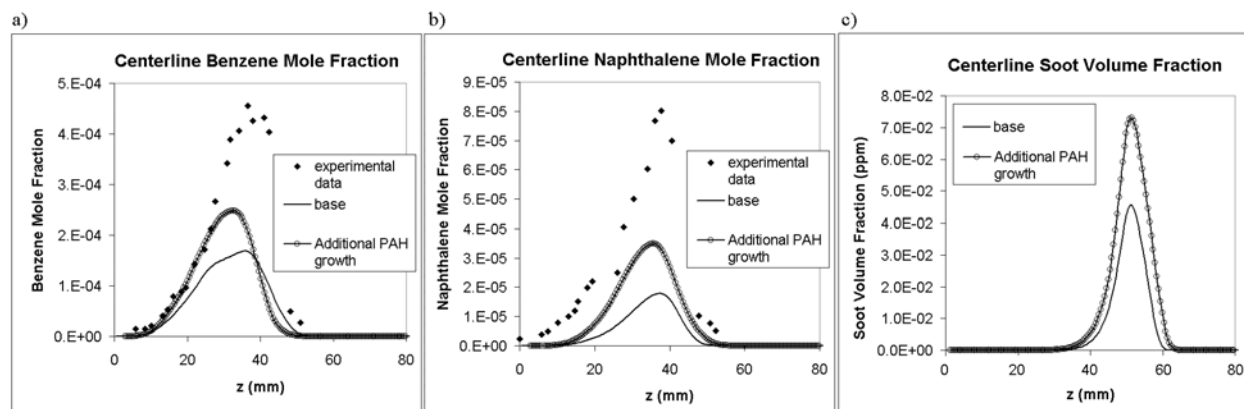


Fig. 3. Comparison of experimental and computed concentrations for the “base” model and the model with additional PAH growth: a) benzene mole fraction, b) naphthalene mole fraction, c) Soot volume fraction.

4. Conclusions

The literature demonstrates a consistent underprediction of soot concentrations in the central/pyrolysis region of coflow laminar diffusion flames. Three common simplifications, which could contribute to this underprediction are tested: neglecting thermal diffusion of large aromatic species that contribute to soot inception; neglecting the formation and growth of polyynes and polyyne-based soot inception; and neglecting PAH growth pathways that fall outside the realm of HACA addition, namely, cyclopentadiene, indene, and propargyl addition.

The effect of neglecting thermal diffusion was studied by performing two computations, one of a coflow laminar diffusion ethylene/air flame with thermal diffusion for H and H₂ only, and one of the same flame with thermal diffusion for all species. The effect of thermal diffusion on soot formation in the central pyrolysis region of the flame was minimal. In fact, the effect was opposite that which was anticipated. Inclusion of thermal diffusion lowered soot concentrations along the centerline. Net thermal diffusion of pyrene, the incepting species in the model was away from the centerline rather than toward it.

Subsequently, the effect of neglecting polyyne chemistry and polyyne-based inception was studied by performing a third computation of the same coflow laminar diffusion ethylene/air flame with polyyne formation, polyyne growth, and polyyne-based inception added to the model. Here too, the effect was opposite that which was anticipated, lowering soot concentrations along the centerline. Consideration of polyynes in the chemical kinetic mechanism drew carbon out of the PAH formation pathways and reduced the centerline concentration of pyrene, the principal incepting species. The increase in soot inception stemming from polyyne growth was more than offset by the reduction in pyrene concentrations.

Finally, a test was conducted on the effect of alternative PAH formation pathways in both the counterflow and coflow geometry. Two counterflow computations were performed, one with a base chemistry set considering only HACA growth of PAHs, and one with an augmented chemistry set considering cyclopentadiene combination, cyclopentadiene-indene combination, and propargyl addition. The augmented chemistry set increased PAH concentrations but naphthalene and pyrene concentrations were still significantly lower than measured data. The same two chemistry sets were implemented in a coflow diffusion flame. Again, the computation with the augmented chemistry set predicted increases in centerline PAH concentrations, which led to an increase in centerline soot formation, but the computed values were still considerably less than the experimental values.

Acknowledgements

The authors acknowledge the Natural Sciences and Engineering Research Council of Canada (NSERC) and the Ontario Ministry of Research and Innovation for financial support, and the SciNet Consortium for providing computational resources.

References

- [1] B.S. Haynes, H.Gg. Wagner, Soot Formation, *Prog. Energy Combust. Sci.* 7 (1981) 229-273.
- [2] K.H. Homann, Formation of Large Molecules, Particulates and Ions in Premixed Hydrocarbon Flames; Progress and Unresolved Questions, *Proc. Combust. Inst.* 20 (1984) 857-870.
- [3] H. Bockhorn, (ed.), *Soot Formation in Combustion: Mechanisms and Models*, Springer-Verlag, Berlin, 1994.
- [4] J. Appel, H. Bockhorn, M. Frenklach, Kinetic Modeling of Soot Formation with Detailed Chemistry and Physics: Laminar Premixed Flames of C₂ Hydrocarbons, *Combust. Flame* 121 (2000) 122-136.

- [5] E. Ranzi, A Wide-Range Kinetic Modeling Study of Oxidation and Combustion of Transportation Fuels and Surrogate Mixtures, *Energ. Fuel.* 20 (2006) 1024-1032.
- [6] Q. Zhang, H. Guo, F. Liu, G. Smallwood, M.J. Thomson, Implementation of an Advanced Fixed Sectional Aerosol Dynamics Model with Soot Aggregate Formation in a Laminar Methane/Air Coflow Diffusion Flame, *Combust. Theor. Model.* 12:4 (2008) 621-641.
- [7] Q. Zhang, H. Guo, F. Liu, G. Smallwood, M.J. Thomson, Modeling of Soot Aggregate Formation and Size Distribution in a Laminar Ethylene/Air Coflow Diffusion Flame with Detailed PAH Chemistry and an Advanced Sectional Aerosol Dynamics Model, *Proc. Combust. Inst.* 32 (2009) 761-768.
- [8] A. Ern, C.C. Douglas, M.D. Smooke, Detailed Chemistry Modeling of Laminar Diffusion Flames on Parallel Computers, *Int. J. Supercomput. Appl.* 9 (1995) 167-186.
- [9] M.D. Smooke, M.B. Long, B.C. Connelly, M.B. Colket, R.J. Hall, Soot Formation in Laminar Diffusion Flames, *Combust. Flame* 143 (2005) 613-628.
- [10] S.B. Dworkin, M.D. Smooke, V. Giovangigli, The Impact of Detailed Multicomponent Transport and Thermal Diffusion Effects on Soot Formation in Ethylene/Air Flames, *Proc. Comb. Inst.* 32 (2009) 1165-1172.
- [11] J.Z. Wen, M.J. Thomson, M.F. Lightstone, S.N. Rogak, Detailed Kinetic Modeling of Carbonaceous Nanoparticle Inception and Surface Growth during the Pyrolysis of C_6H_6 behind Shock Waves, *Energy & Fuels* 20 (2006) 547-559.
- [12] A. D'Anna, J.H. Kent, Modeling of Particulate Carbon and Species Formation in Coflowing Diffusion Flames of Ethylene, *Combust. Flame* 144 (2006) 249-260.
- [13] N.M. Marinov, W.J. Pitz, C.K. Westbrook, A.M. Vincitore, M.J. Castaldi, S.M. Senkan, Aromatic and Polycyclic Aromatic Hydrocarbon Formation in a Laminar Premixed n-Butane Flame, *Combust. Flame* 114 (1998) 192-213.
- [14] R.J. Santoro, H.G. Semerjian, R.A. Dobbins, Soot Particle Measurements in Diffusion Flames, *Combust. Flame* 51 (1983) 203-218.
- [15] Q. Zhang, Detailed Modeling of Soot Formation/Oxidation in Laminar Coflow Diffusion Flames, PhD thesis, University of Toronto, Toronto, Canada, 2009.
- [16] S.H. Park, S.N. Rogak, W.K. Bushe, J.Z. Wen, M.J. Thomson, An Aerosol Model to Predict Size and Structure of Soot Particles, *Combust. Theor. Model.* 9 (2005) 499-513.
- [17] S.J. Harris, A.M. Weiner, Soot Particle Growth in Premixed Toluene/Ethylene Flames, *Combust. Sci. Technol.* 38 (1984) 75-84.
- [18] K.G. Neoh, J.B. Howard, A.F. Sarofim, Soot Oxidation in Flames," in D.C. Seigla and G.W. Smith (eds.), *Particulate Carbon: Formation During Combustion*, Plenum, New York, 1981.
- [19] F. Xu, P.B. Sunderland, G.M. Faeth, Soot Formation in Laminar Premixed Ethylene/Air Flames at Atmospheric Pressure, *Combust. Flame*, 108 (1997) 471-493.
- [20] F. Liu, G.J. Smallwood, O.L. Gülder, Band Lumping Strategy for Radiation Heat Transfer Calculations Using a Narrowband Model, *J. Thermophys. Heat Transfer*, 14:2 (2000) 278-281.
- [21] S.V. Patankar, *Numerical Heat Transfer and Fluid Flow*, Hemisphere, New York, 1980.
- [22] R.J. Kee, J.A. Miller, T.H. Jefferson, Chemkin: A General Purpose, Problem Independent, Transportable, Fortran Chemical Kinetics Code Package, Report SAND80-8003, 1980.
- [23] R.J. Kee, F.M. Rupley, J.A. Miller, A Fortran chemical kinetics package for the analysis of gas-phase chemical kinetics, Sandia Report SAND89-8009, 1989.
- [24] R.J. Kee, J. Warnatz, J.A. Miller, A Fortran Computer Code Package for the Evaluation of Gas-Phase Viscosities, Conductivities, and Diffusion Coefficients, Report SAND82-8209, 1983.
- [25] R.J. Kee, G. Dixon-Lewis, J. Warnatz, M.E. Coltrin, J.A. Miller, A Fortran Computer Code Package for the Evaluation of Gas-Phase Multicomponent Transport Properties, Report SAND86-8246, 1986.
- [26] D.E. Keyes, M.D. Smooke, Flame Sheet Starting Estimates for Counterflow Diffusion Flame Problems, *J. Comput. Phys.* 73 (1987) 267- 288.
- [27] N. Olten, S. Senkan, Formation of Polycyclic Aromatic Hydrocarbons in an Atmospheric Pressure Ethylene Diffusion Flame, *Combust. Flame* 118 (1999) 500-507.
- [28] R.J. Kee, F.M. Rupley, J.A. Miller, M.E. Coltrin, J.F. Grcar, E. Meeks, H.K. Moat, A.E. Lutz, G. Dixon-Lewis, M.D. Smooke, J. Warnatz, G.H. Evans, R.S. Larson, R.E. Mitchell, L.R. Petzold, W.C. Reynolds, M. Caracotsios, W.E. Stewart, P. Glarborg, C. Wang, C.L. McLellan, O. Adigun, W.G. Houf, C.P. Chou, S.F. Miller, P. Ho, P.D. Young, D.J. Young, D.W. Hodgson, M.V. Petrova, K.V. Puduppakkam, CHEMKIN release 4.1. San Diego, California 2006.
- [29] C.S. McEnally, L.D. Pfefferle, Experimental Study of Nonfuel Hydrocarbons and Soot in Coflowing Partially Premixed Ethylene/Air Flames, *Combust. Flame* 121 (2000) 575-592.